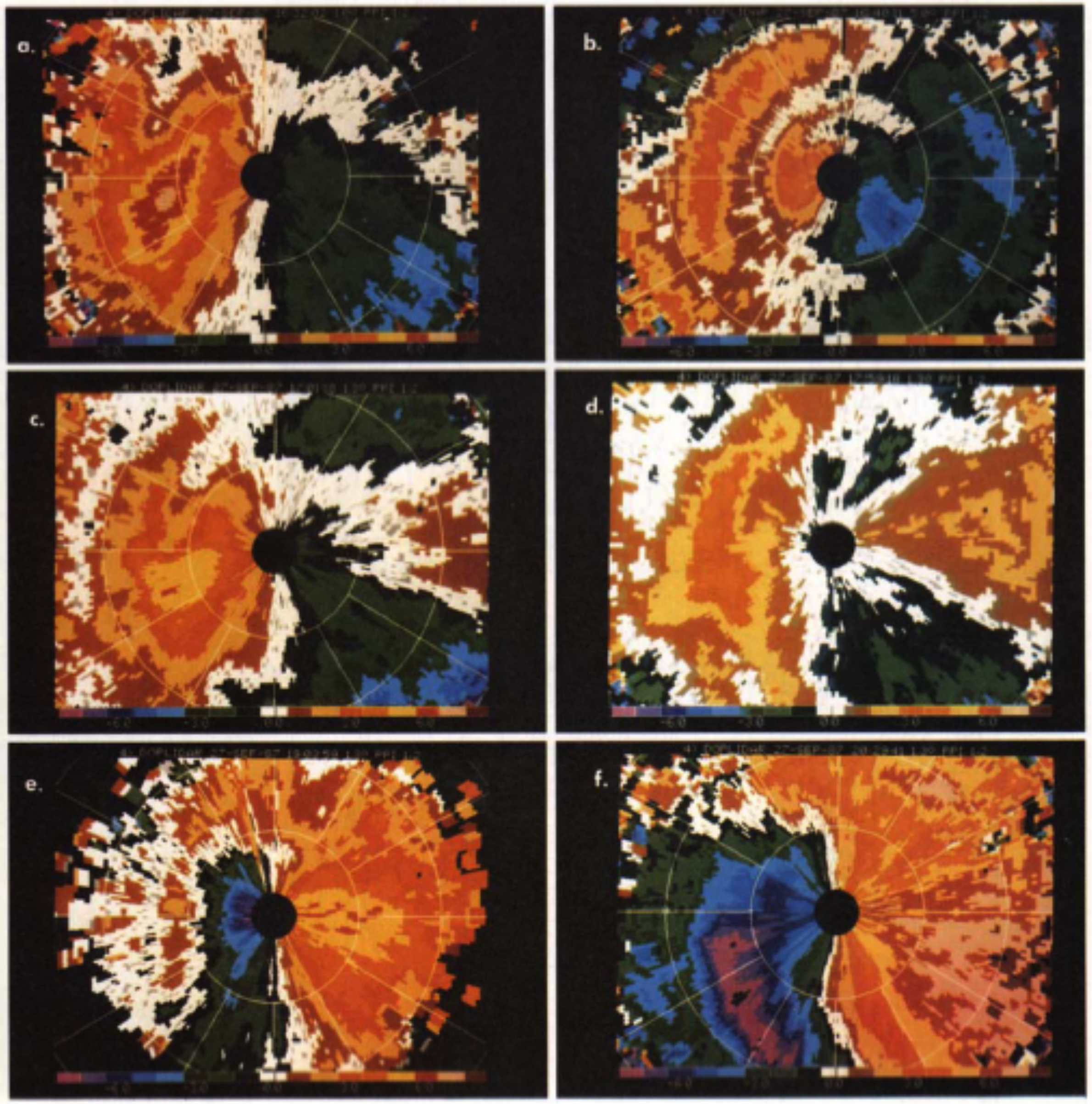

FIG. 3. Lidar PPI scans of radial velocity (m s^{-1}), depicting the evolution from land breeze to sea breeze. The lidar is in the center of each scan, and the indicated minimum range is 1.5 km. North is to the top, Monterey Bay to the left (west), and land (east) to the right. Range rings are 5 km apart and azimuth rays are every 30°. Negative velocities, represented by purple, blue, and green colors indicate flow toward the lidar. Positive velocities (tan, yellow, red) indicate flow away from the lidar. The time and elevation angle of each scan is as follows: (a) 1632:02 UTC, 1.0°; (b) 1640:11 UTC, 5°; (c) 1701:18 UTC, 1.3°; (d) 1759:18 UTC, 1.3°; (e) 1903:59 UTC, 1.3°; (f) 2029:41 UTC 1.3°. At 1.3° elevation, the 5-km range ring is at a height of 436 m and the 10-km range ring is at a height of 872 m.

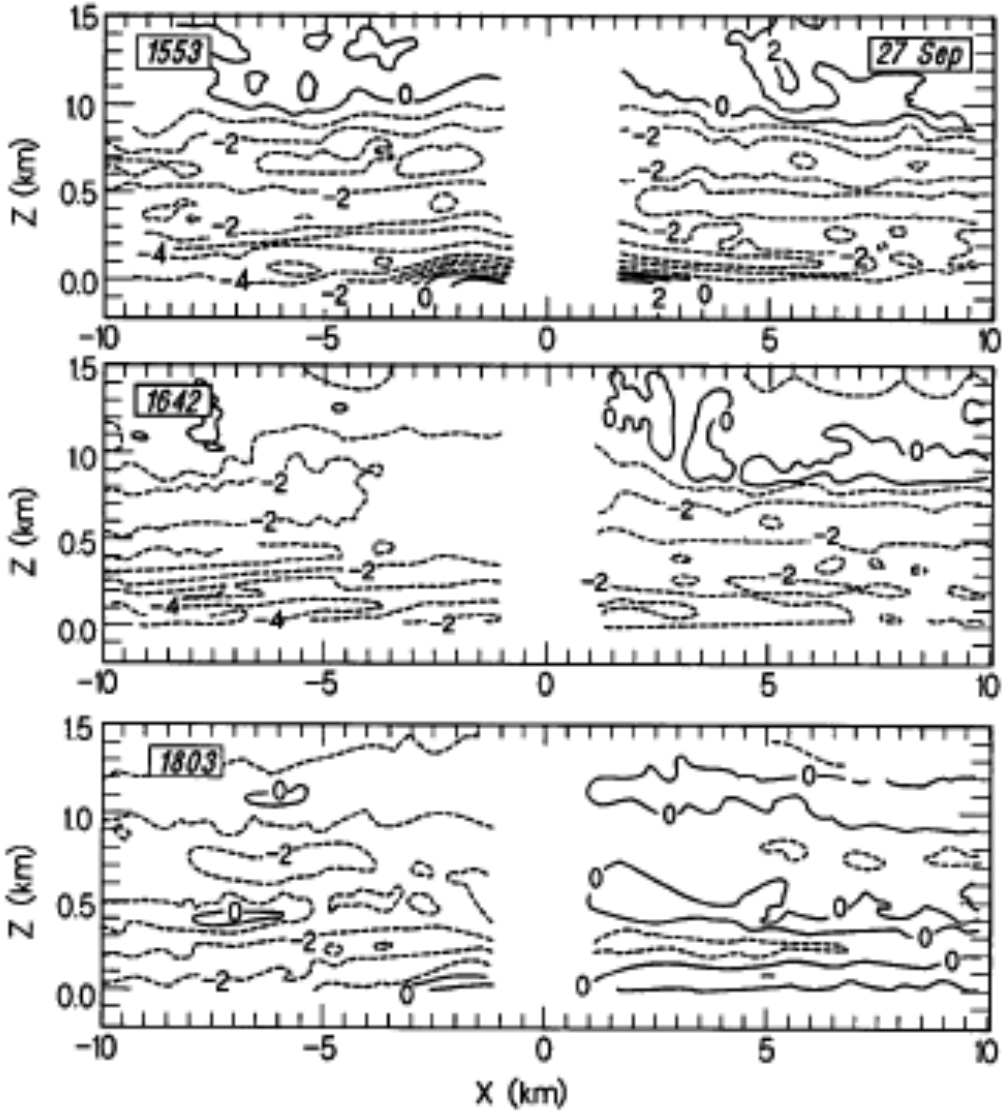

FIG. 4. Vertical cross sections of the u component of the wind on 27 September. The lidar is positioned at (0, 0), 1.5 km east of the shore. Monterey Bay is to the left, land to the right. Dashed lines indicate easterly flow and solid lines indicate westerly flow. Time (UTC) of the plot is in the upper left-hand corner. (a) Offshore flow of 1-km depth at 1553 UTC (0753 PST) with a "minor sea breeze" at the surface, near the shore. (b) Offshore flow at 1642 UTC (0842 PST). (c) Light westerly flow at the surface (sea breeze) underlying weakening offshore flow at 1803 UTC (1003 PST). Grid spacing was 100 m in the horizontal and 25 m in the vertical.

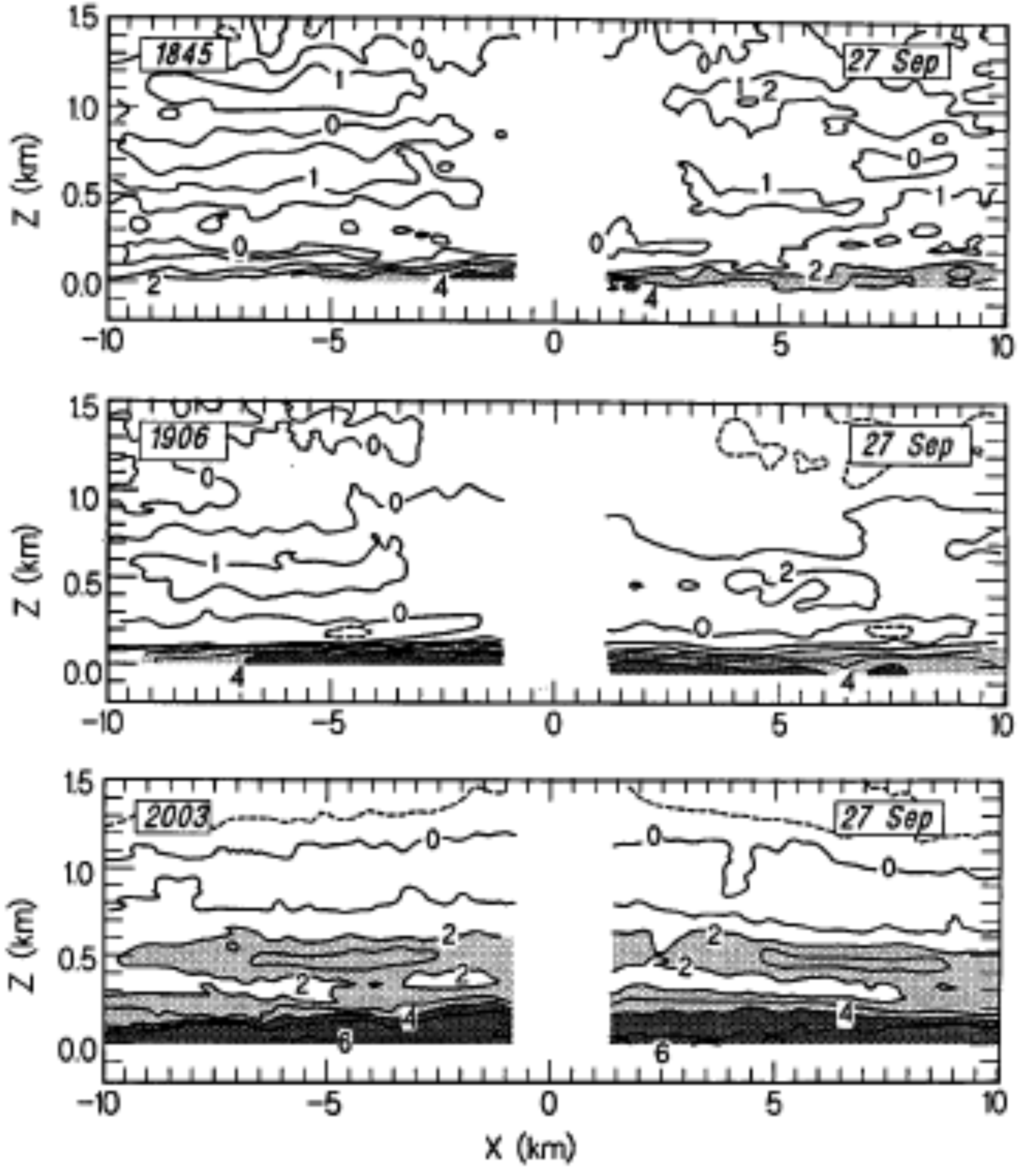

FIG. 5. As in Fig. 4, starting 42 min after Fig. 4c. The westerly, sea-breeze flow now extended up to 1.5 km, with the strongest winds near the surface. The sea breeze steadily increased in speed and became more well defined with time as illustrated at (a) 1845 UTC (1045 PST), (b) 1906 UTC (1106 PST), and (c) 2003 UTC (1203 PST). Light shading indicates flow over 2 m s^{-1}; dark shading, over 4 m s^{-1}.

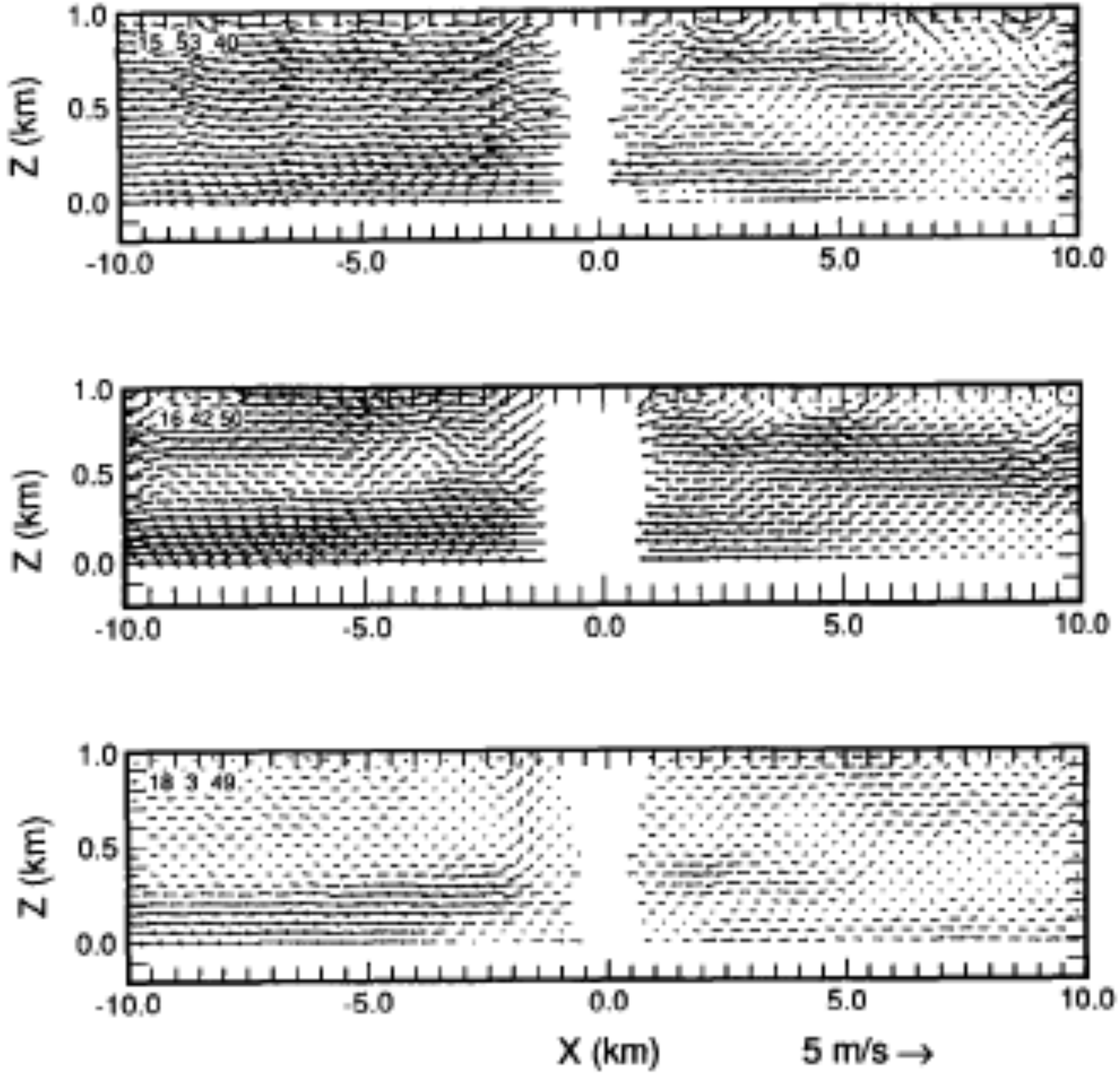

FIG. 6. Vector plots of the u and w components of the wind from the same scans seen in Fig. 4.

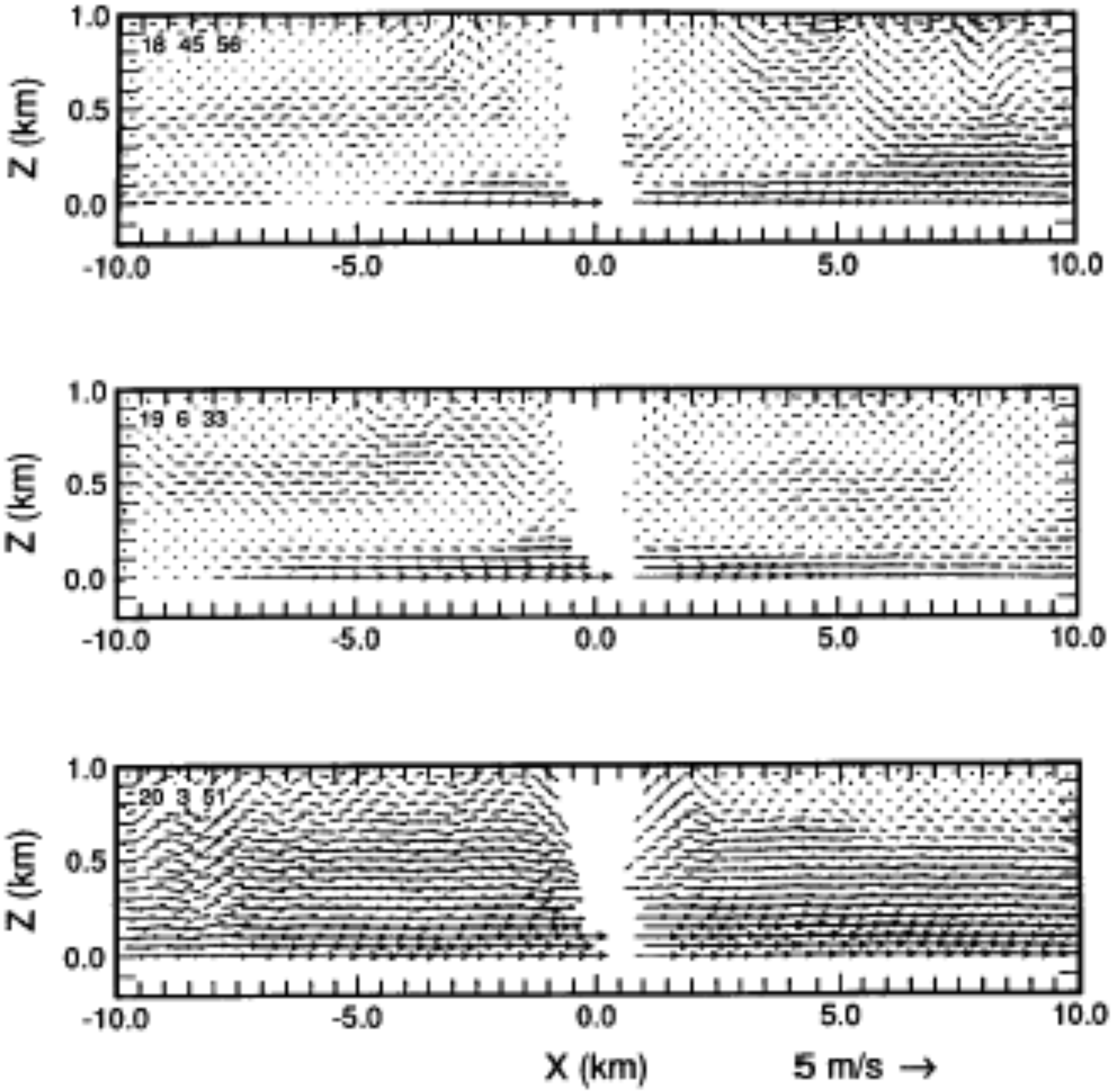

FIG. 7. Vector plots of the *u* and *w* components of the wind from the same scans seen in Fig. 5.

“VORTICITY THINKING”

$$\omega = \nabla \mathbf{X}\ \mathbf{v} = (\underset{x}{\xi},\ \underset{y}{\eta},\ \underset{z}{\zeta})$$

$$\nabla \mathbf{X}\ (D\mathbf{v}/Dt = \mathrm{PGF} + B\ \mathbf{k})$$

$$D\omega/Dt = \omega \bullet \nabla \mathbf{v} + \nabla \mathbf{X}\ B\ \mathbf{k}$$

CONVERGENCE/
DIVERGENCE/
TILTING

BUOYANCY
GRADIENTS/
BAROCLINIC EFFECT

$$(-\boldsymbol{k}\ \mathrm{X}\ \nabla B)$$

$D\eta/Dt = -\,\partial B/\partial x \qquad (\partial/\partial y = 0,\ v = 0)$

$\eta = \partial u/\partial z - \partial w/\partial x$

$\partial u/\partial x + \partial w/\partial z = 0$ CONTINUITY

$\eta = \partial^2\psi/\partial x^2 + \partial^2\psi/\partial z^2$

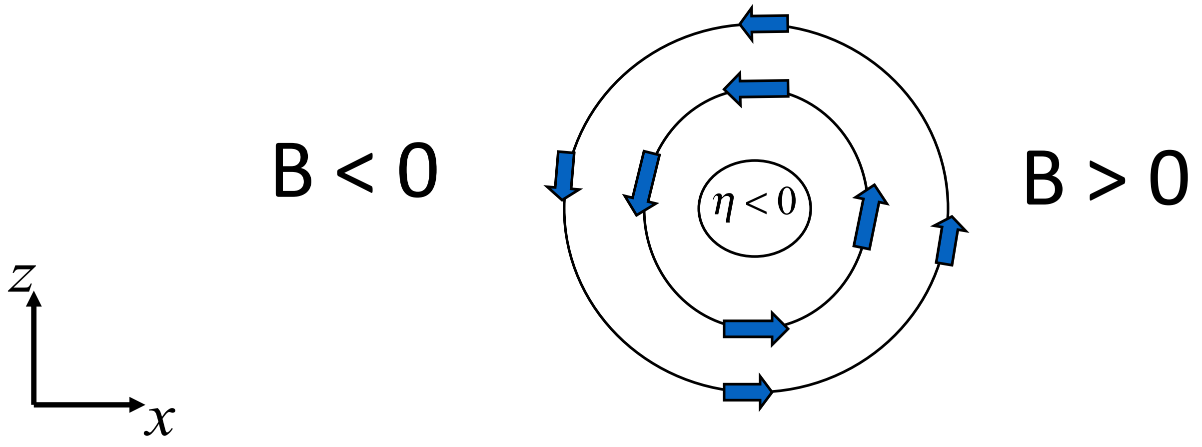

SOLENOIDAL GENERATION OF HORIZONTAL VORTICITY ON A NON-SLOPING SURFACE

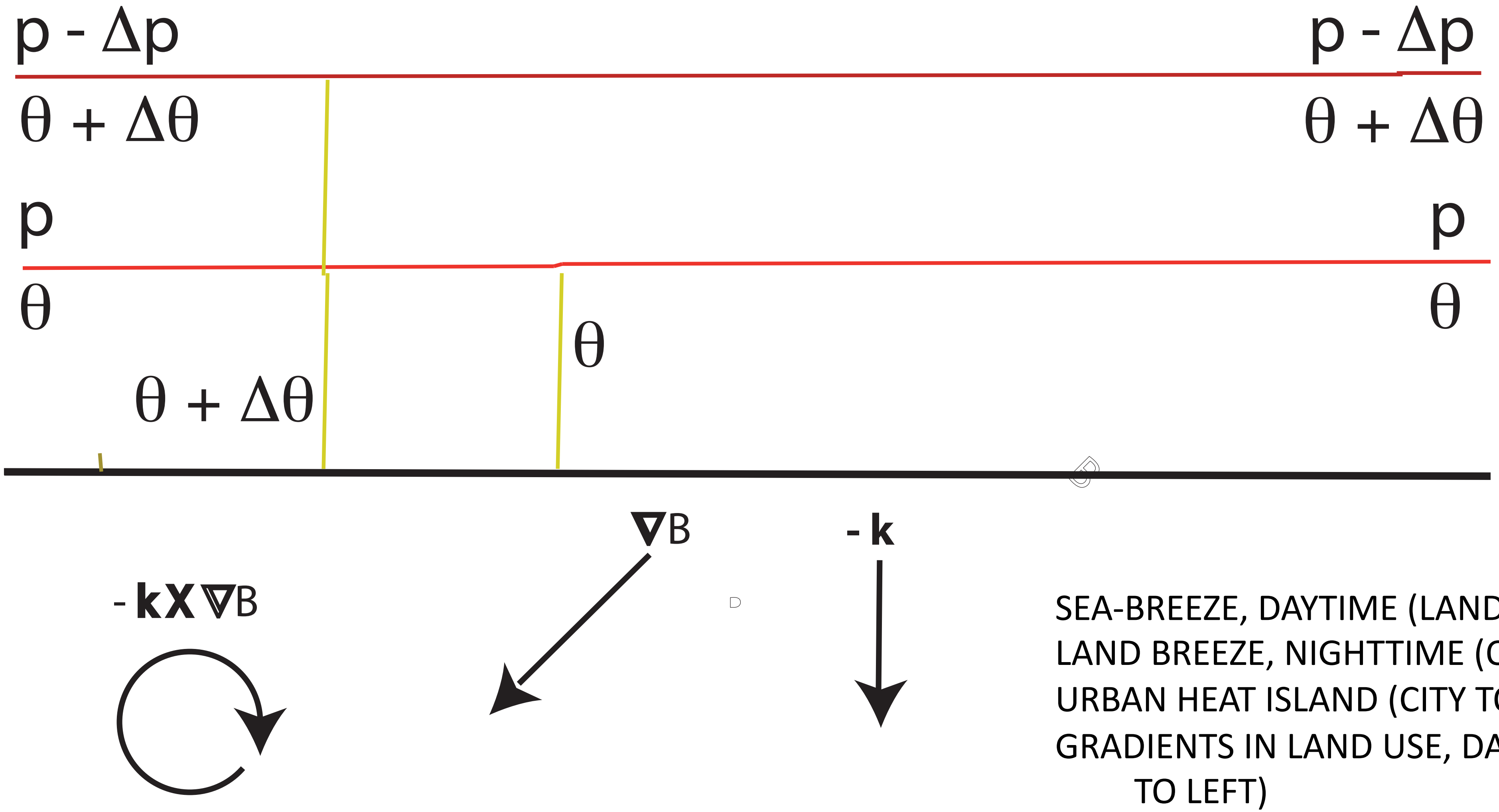

SEA-BREEZE, DAYTIME (LAND TO LEFT)
LAND BREEZE, NIGHTTIME (OCEAN TO LEFT)
URBAN HEAT ISLAND (CITY TO LEFT)
GRADIENTS IN LAND USE, DAY (DRIER LAND TO LEFT)

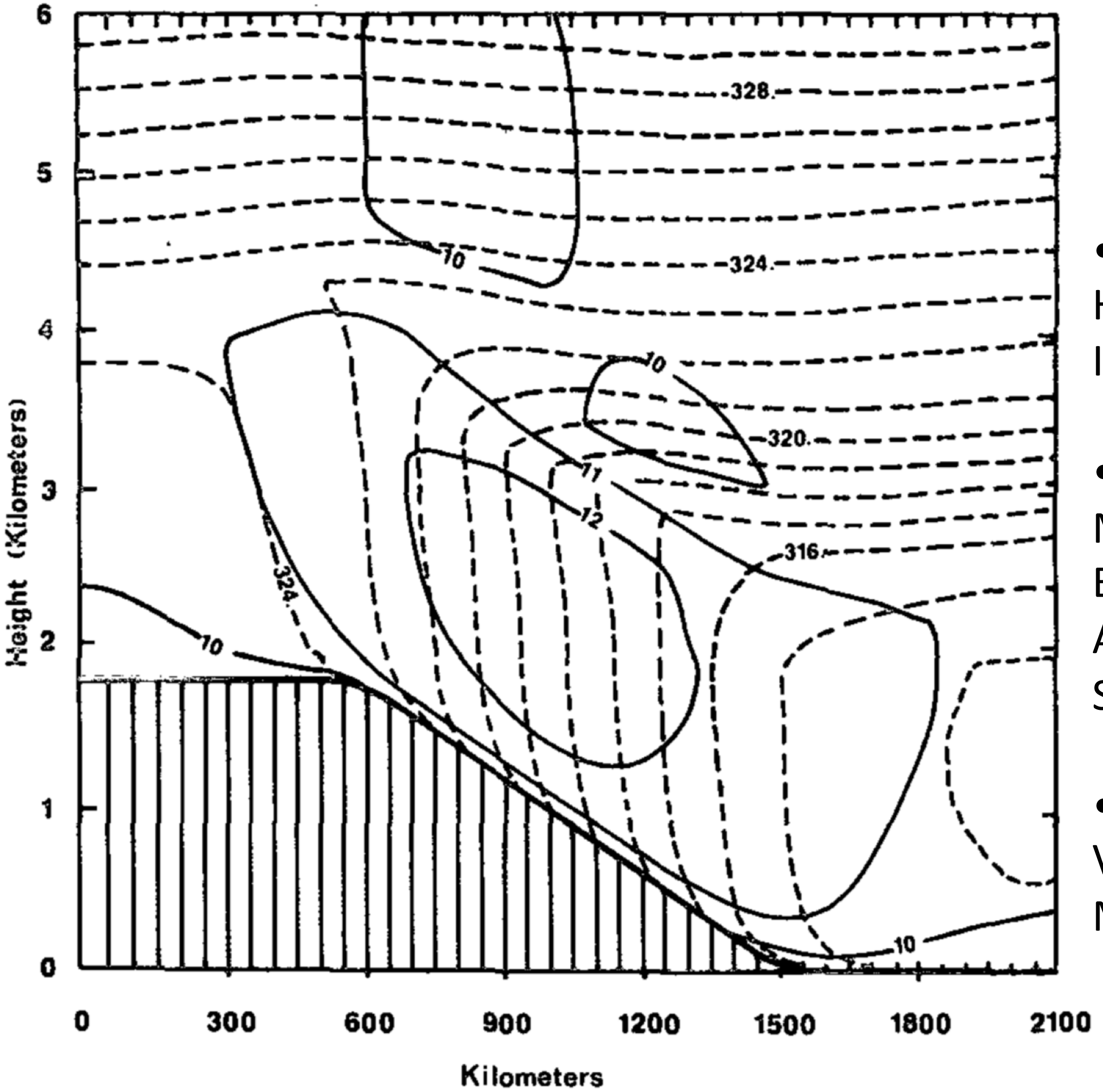

FIG. 12. Composite v component (solid) and potential temperature (dashed) contours at 1500 LST showing the development of the convective boundary layer and baroclinic zone over the sloping terrain for case 1. Contour intervals are 1 m s^{-1} and 1 K.

- EFFECTS OF SFC HEAT FLUX DUE TO INSOLATION
- EFFECTS OF VERTICAL MIXING (CAN HAPPEN EVEN AT NIGHT IN THE ABSENCE OF UPWARD SFC HEAT FLUX)
- NEGLECT GRADIENTS OF VEGETATION,SOIL MOISTURE, ETC.

McNider and Pielke 1981, *JAS*

SOLENOIDAL GENERATION OF HORIZONTAL VORTICITY ON A SLOPING SURFACE

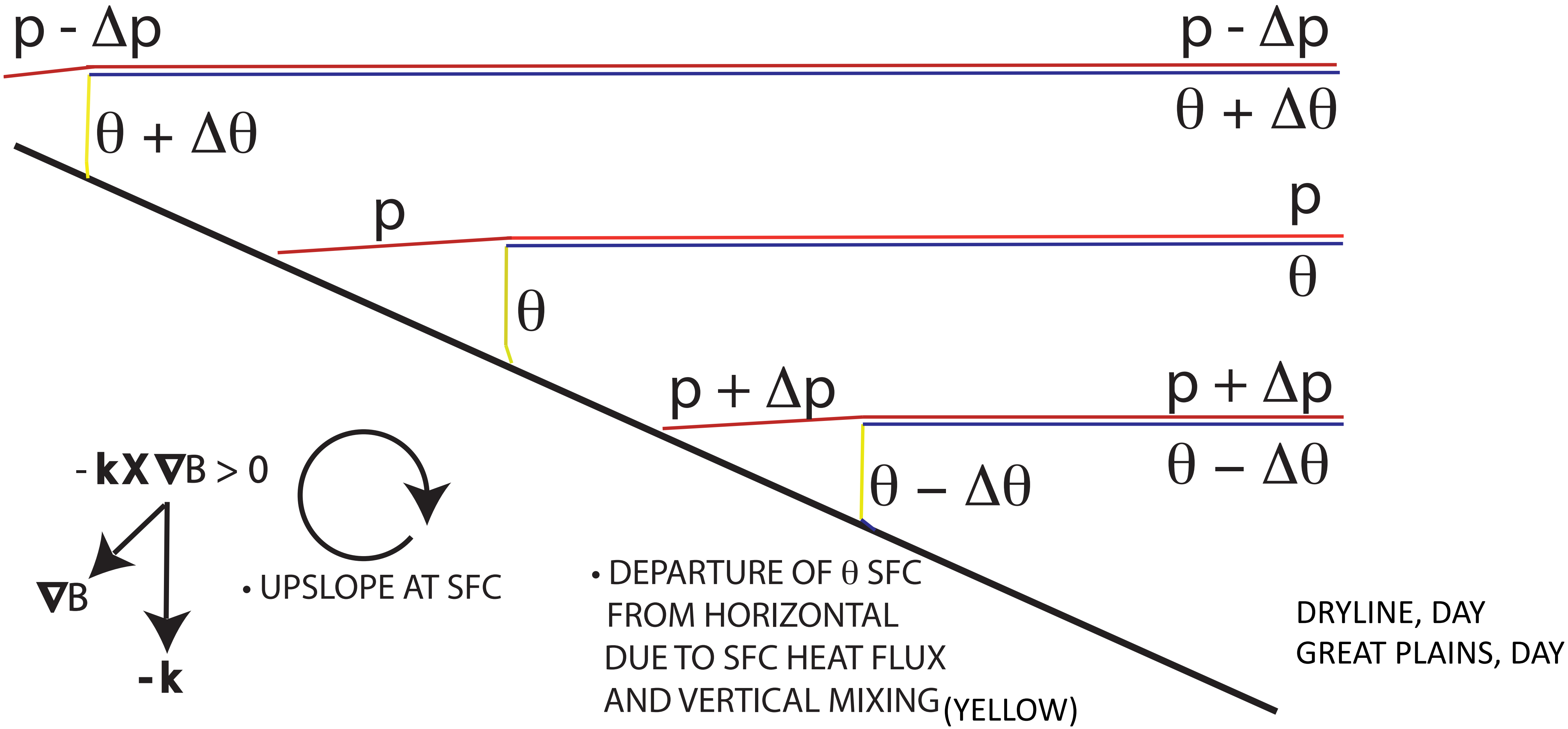

VERTICAL CROSS SECTION: X-TO RIGHT, Y-INTO FIGURE

Bluestein et al. 2018, MWR

SOLENOIDAL GENERATION OF HORIZONTAL VORTICITY ON A HIGHLY SLOPING SURFACE

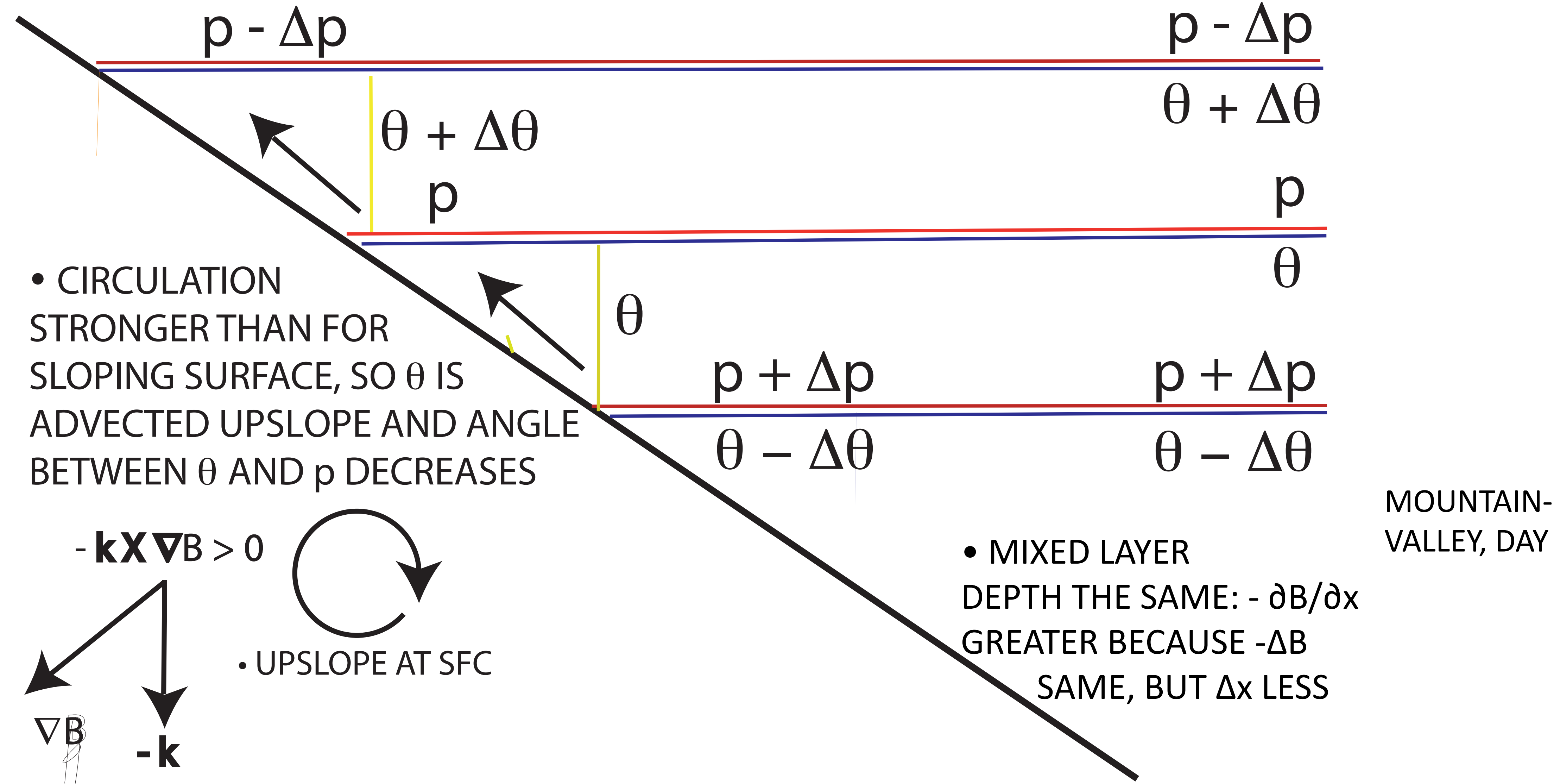

• CIRCULATION STRONGER THAN FOR SLOPING SURFACE, SO θ IS ADVECTED UPSLOPE AND ANGLE BETWEEN θ AND p DECREASES

• UPSLOPE AT SFC

• MIXED LAYER DEPTH THE SAME: - ∂B/∂x GREATER BECAUSE -ΔB SAME, BUT Δx LESS

- AS SLOPE OF GROUND DECREASES, ANGLE BETWEEN $\nabla \mathbf{B}$ AND -$\mathbf{k}$ DECREASES ($\nabla \mathbf{B}$ BECOMES MORE VERTICAL), SO $\partial\eta/\partial t$ DECREASES

- AS SLOPE INCREASES, ANGLE BETWEEN $\nabla \mathbf{B}$ AND –$\mathbf{k}$ INCREASES ($\nabla \mathbf{B}$ BECOMES MORE HORIZONTAL AND STRONGER), SO VERTICAL CIRCULATION INTENSIFIES, BUT….

w COMPONENT OF MOTION ASSOCIATED WITH VERTICAL CIRCULATION MODIFIES $\nabla \mathbf{B}$ AS $\partial B/\partial t = - N^2 w$, SO INSENTROPES BECOME MORE HORIZONTAL AND $\nabla \mathbf{B}$ BECOMES MORE VERTICAL, WHICH ACTS AS A BRAKE ON $\partial\eta/\partial t$ (LIKE LE CHATELIER’S PRINCIPLE!)

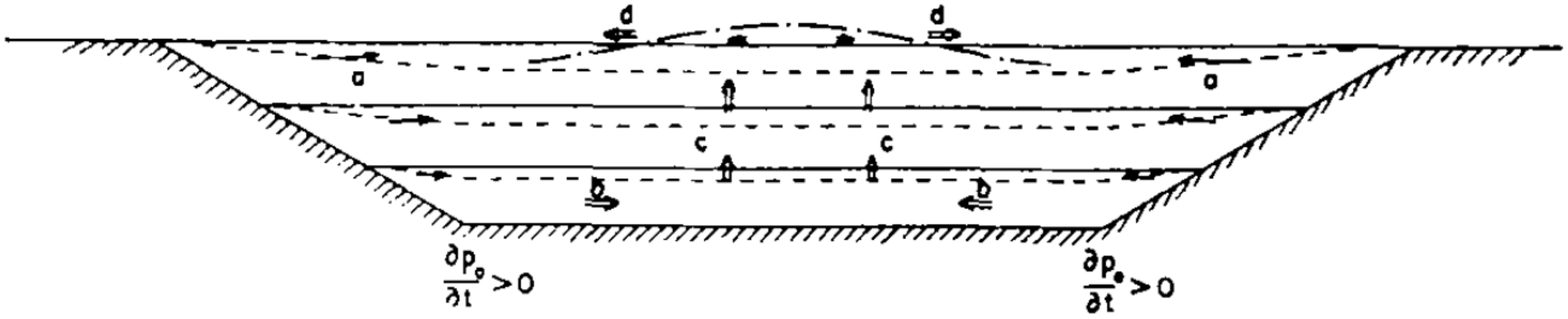

Figure 2. Idealized scheme of the circulation developing during the night.

DRAINAGE WIND AT NIGHT AND REVERSE DRAINAGE WIND DURING THE DAY

Bleeker and Andre 1951, *QJRMS*